

Published in final edited form as:

J Orthop Sci. 2009 May ; 14(3): 298–306. doi:10.1007/s00776-009-1325-z.

In vivo anterior cruciate ligament elongation in response to axial tibial loads

Ali Hosseini^{1,2}, Thomas J. Gill¹, and Guoan Li¹

¹Bioengineering Laboratory, Department of Orthopaedic Surgery, Massachusetts General Hospital/Harvard Medical School, 55 Fruit Street, GRJ 1215, Boston, MA 02114, USA

²Department of Mechanical Engineering, Massachusetts Institute of Technology, Cambridge, MA, USA

Abstract

Background—The knowledge of in vivo anterior cruciate ligament (ACL) deformation is fundamental for understanding ACL injury mechanisms and for improving surgical reconstruction of the injured ACL. This study investigated the relative elongation of the ACL when the knee is subject to no load (<10 N) and then to full body weight (axial tibial load) at various flexion angles using a combined dual fluoroscopic and magnetic resonance imaging (MRI) technique.

Methods—Nine healthy subjects were scanned with MRI and imaged when one knee was subject to no load and then to full body weight using a dual fluoroscopic system (0°–45° flexion angles). The ACL was analyzed using three models: a single central bundle; an anteromedial and posterolateral (double functional) bundle; and multiple (eight) surface fiber bundles.

Results—The anteromedial bundle had a peak relative elongation of $4.4\% \pm 3.4\%$ at 30° and that of the posterolateral bundle was $5.9\% \pm 3.4\%$ at 15°. The ACL surface fiber bundles at the posterior portion of the ACL were shorter in length than those at the anterior portion. However, the peak relative elongation of one posterolateral fiber bundle reached more than 13% whereas one anteromedial fiber bundle reached a peak relative elongation of only about 3% at 30° of flexion by increasing the axial tibial load from no load to full body weight.

Conclusions—The data quantitatively demonstrated that under external loading the ACL experiences nonhomogeneous elongation, with the posterior fiber bundles stretching more than the anterior fiber bundles.

Introduction

The anterior cruciate ligament (ACL) is frequently injured in sports and during strenuous activities, especially in younger populations.^{1,2} The importance of ACL injury to public health has led to numerous investigations of ACL material properties and structural functions.^{3,4} Many investigations have reported on the force–elongation relation^{4–6} and stress–strain behavior³ of the ACL to try to understand the biomechanical properties of the ligament. These studies were usually conducted using uniaxial tensile tests on ACL specimens,^{3,4,7} where the ACL was considered in different structural configurations such as a single tension element⁴; two-bundle elements³; or multibundle elements.^{3,7} Furthermore, numerous in vitro investigations have measured ACL forces in response to various loads applied to the knee to understand the biomechanical function of the ligament in the knee

joint.^{2,8,9} These investigations used various measurement techniques, such as a buckle transducer,¹⁰ implantable pressure transducer,⁸ Hall effect strain transducer,^{11,12} and a robotic technique.^{9,13–15} Among these various ACL biomechanical studies, most have determined the ACL forces by applying an anterior tibial load.^{2,15,16} Few studies also measured ACL forces under rotational moments^{17,18} or simulated muscle loads.^{13,19} Although these data have markedly improved our knowledge of ACL biomechanics, quantitative determination of the ACL function under in vivo physiological loading conditions is still a challenge in biomedical engineering research.

Early investigations on in vivo ACL biomechanics have used strain-gauge techniques to measure the elongation of the ACL in living subjects.⁸ Beynnon et al. conducted direct measurements of ACL strains in the anterior portion of the ligament using a differential variable reluctance transducer (DVRT) during various in vivo activities of the knee.¹² Li et al.²⁰ and Jordan et al.²¹ measured the elongation pattern of the ACL using a noninvasive imaging modality during weight-bearing flexion of the knee. These studies indicated that the ACL may function in a more complicated three-dimensional (3D) manner. This knowledge is critical for understanding the in vivo loading effect on ACL function and ACL injury mechanisms as well as for optimizing surgical treatment of the injured ACL.

The objective of this study was to investigate the elongation behavior of the healthy ACL under weight-bearing conditions in living subjects. Because of the complicated anatomical structure of the ACL and its 3D deformation in nature, for an anatomical ACL reconstruction the ACL biomechanics in different regions of the ligament must be considered. Therefore, we simulated the ACL using a more detailed anatomical approach: (1) a single central bundle; (2) double functional bundles; and (3) multiple surface fiber bundles. A combined dual fluoroscopic and magnetic resonance imaging (MRI) technique was used to determine relative elongations of ACL bundles at different flexion angles when the tibia was loaded from no load (<10 N) to full body weight (BW).

Materials and methods

Nine subjects (four males, five females), aged 23–48 years old, were recruited with the approval of the institutional review board (IRB). All subjects had normal, healthy knees with no history of injury or surgery (determined by both clinical examination and MRI examination). Written informed consent was obtained from all subjects prior to their participating in this study.

Magnetic resonance imaging and 3D knee models

Each knee (chosen randomly, five right and four left knees) was scanned in a relaxed, full extension position using a 3.0 T MR Scanner (Trio; Siemens, Malvern, PA, USA). The knee was scanned in both sagittal and coronal planes in 1 mm slice thickness using a 3D double echo water excitation sequence.^{20,22} The size of the MR images was 160 × 160 mm with a resolution of 512 × 512 pixels. The series of MR images were imported into solid modeling software (Rhinoceros; Robert McNeel, Seattle, WA, USA) for construction of 3D models of the knee (Fig. 1). The bony contours were segmented in MR images, and the 3D anatomical models of the bones were created using the digitized contour data.

The attachment areas of the ACL on the femur and tibia were segmented on MR images in both sagittal and coronal planes. Because the ACL insertion sites were segmented in the same coordinate setup as that for segmentation of the femur and tibia, these attachment areas were directly mapped onto the 3D anatomical model of the knee (Fig. 2A). The attachment areas were further divided into two parts: (AM) and posterolateral (PL) bundle attachment areas of the ACL (Fig. 2C). This was done by an orthopedic surgeon because there are no

distinct separations between the AM and PL bundle insertion sites on the tibia and femur that could be specified from the MR images. The geometrical centers of the attachment areas of each bundle were determined as in previous studies.²¹ The AM and PL attachment site geometry on both tibial and femoral sides were then compared to previous anatomical studies to make sure that the determination of the bundles was consistent with previous studies.^{21,23–25}

To investigate the 3D elongation of the ACL, we further divided the boundaries of the ACL insertion sites into eight divisions (Fig. 2C). On the tibial attachment site, points 1–4 were chosen on the anteromedial section of the ACL such that point 1 was always placed on the lateral border of the AM and PL bundles and the numbers assigned to the points increased when moving medially (Fig. 2C). Similarly, points 5–8 were chosen on the posterolateral section of the ACL attachment site such that point 5 was placed on the medial border of the AM and PL bundles and the number assigned to the points increased by moving laterally (Fig. 2C). The points were evenly distributed along the ACL attachment boundaries. The femoral insertion site has been treated in a similar way.

The arrangement of the points is the same for right and left knees. Each point on the tibial attachment area has been connected to its corresponding point on the femoral side, and the resulting lines were defined as surface fiber bundles of the ACL and were numbered the same as its end points for studying the nonhomogeneous elongation of the surface fiber bundles of the ACL (Fig. 2C). A cadaveric specimen was dissected to verify the reconstructed ACL model qualitatively (Fig. 2B). The configuration of the ACL was shown to twist externally in the tibial attachment relative to the femoral attachment site in both the reconstructed ACL model and the cadaveric ACL.

Fluoroscopic imaging of the knee

A dual fluoroscopic system²⁶ has been used to capture the joint positions along the flexion path of the knee (Fig. 3A). The system setup consists of two fluoroscopes (BV Pulsera; Philips, Bothell, WA, USA) that were positioned orthogonally to each other. A force plate constructed using a 6 degrees-of-freedom (DOF) load sensor (JR3, San Francisco, CA, USA) was installed on the top of the platform and was connected to a monitor to display simultaneously the value of ground reaction forces when the subject steps on the force plate (Fig. 3A).

The subject first stood on the force plate on both feet in a relaxing position for measurement of body weight. The subject then put only the testing leg on the force plate. The body weight load applied on the testing leg could be controlled by the subject through the force plate output that was displayed on the monitor. In this experiment, each subject was tested under the no load condition (<10 N) and full body weight condition and at four flexion angles: 0°, 15°, 30°, 45°.

At each target flexion angle, the subject was asked to step on the force plate using the testing leg while the force plate measured a minimal load (<10 N) to represent the no-load condition. The fluoroscopes imaged the knee position simultaneously. The subject was then asked to apply full body weight on the testing leg while maintaining the same flexion angle. The subject could reach the target load within 5 s. The fluoroscopes imaged the new position again. After testing at one flexion angle, the subject was asked to flex the knee to the next target flexion angle. The knee was tested in this manner at all target flexion angles from low to high angles. The flexion angle was controlled using a goniometer by a single investigator throughout the experiment. The entire experiment for each subject took approximately 10 min.

Reproducing in vivo knee positions

A virtual dual fluoroscopic system based on the geometry of the actual experimental system was created in 3D solid modeling software (Fig. 3B). The pair of fluoroscopic images of the knee position under a specific tibial load were imported into the software and placed at the positions of the image intensifiers of the virtual system. Two virtual cameras were positioned to represent the actual X-ray sources.

The bony contours of both tibia and femur were outlined on both fluoroscopic images to facilitate matching the 3D anatomical model of the bones with their fluoroscopic images. The 3D anatomical model of the knee was imported into the virtual fluoroscopic system and projected onto the virtual image intensifiers by the virtual cameras. Each bony model was individually manipulated in 6 DOF until the projection of the 3D bony model matched the outline of the bony contours on the fluoroscopic images (Fig. 3B). The in vivo position of the knee captured on the fluoroscopic images was then reproduced using the matched 3D bony models. By repeating the same procedure using the fluoroscopic image pairs obtained at all flexion angles and under all loading conditions, the kinematics of the knee of the subject during the experiment could be reproduced using a series of matched bony models of the knee. Because the attachment areas of the ACL are fixed to the corresponding bony surfaces of the tibia and femur, the relative positions of these attachment areas of the ACL could be determined using the series of matched bony models under different loading conditions and flexion angles. Therefore, the positions of both ends of each bundle of the ACL could be determined.

The accuracy of the above procedure in reproducing knee kinematics has been extensively evaluated.^{22,26} Using standard geometries, the system has an accuracy of 0.1 mm in translation and 0.1° in rotation.²⁶ Using cadaveric human knee specimens, the system has an accuracy of 0.1 mm in translation and a repeatability of 0.3° in rotation.²⁷ The accuracy of determination of knee kinematics can directly affect the accuracy of the ACL elongation data. If the translational accuracy when determining the femoral and tibial positions was 0.1 mm,²⁶ the effect on the accuracy of the ACL bundle elongation was maximally estimated to be 0.34 mm. The average ACL length for all the subjects was ~26 mm. Therefore, the maximum error in relative ACL elongation was estimated to be within a range of ± 0.026, or 2.6%.

Data Analysis

The results of this study can be presented in three portions. First, the ACL was considered as a single ligament using its central bundle. Then, the kinematics of the AM and PL bundles was determined. Finally, the elongations of eight surface fiber bundles of the ACL were determined. The length of the ACL central bundle was defined as the line connecting the ACL attachment centers on the tibia and femur (this line was also defined as the long axis of the ACL). The length of the AM bundle was defined as the line connecting the AM bundle attachment centers on the tibia and femur, and the same was done for the PL bundle. The lengths of the eight lines, connecting each of the eight points on the tibia to their corresponding points on the femur represent the surface fiber bundles of the ACL. To investigate the loading effect on ACL elongation, the length of the ACL bundles under the no-load condition at each flexion angle (l_0) was used as a reference to determine the *relative elongation* of the fiber bundles in response to increased tibial loads at that flexion angle

$$e=(l-l_0)/l_0$$

where l is the length of the ACL bundle under full body loading at that flexion angle.

A two-way repeated-measures analysis of variance (ANOVA) and the Student-Newman-Kuels test were used to compare the ACL deformation. The flexion angle and body weight loading applied to the leg were considered as independent variables and the lengths of ACL fiber bundles as dependent variables. Statistical significance was defined when $P < 0.05$.

Results

Single bundle

In general, the length of the ACL increased with tibial load (Fig. 4A). At full extension, the length of the ligament increased from 27.1 ± 2.3 mm at the no-load condition to 27.5 ± 2.4 mm under full body weight. The increases of the ACL length caused by the full body weight condition were significant at 15° and 30° of flexion ($P < 0.05$).

The relative elongation of the ACL caused by full body weight loading peaked at 15° and 30° of flexion (Fig. 4B). At full extension, full body weight loading caused a relative ACL elongation of $1.2\% \pm 2.2\%$. At 15° and 30° of flexion, full body weight caused relative ACL elongations of $4.5\% \pm 3.2\%$ and $4.6\% \pm 3.3\%$, respectively. The relative ACL elongation dropped to $2.3\% \pm 4\%$ at 45° of flexion. The relative elongation at 15° and 30° were significantly higher than those at 0° and 45° of flexion ($P < 0.05$).

Double bundles

The length patterns of the AM and PL bundles along the flexion path were similar under no-load and full body weight conditions (Fig. 5A, B). The AM bundle increased in length with flexion angles and the PL bundle decreased in length with flexion angles.

By increasing the load from no-load (<10 N) to full body weight, the length of the AM bundle showed a peak relative elongation of $4.4\% \pm 3.4\%$ at 30° of flexion (Fig. 5C). However, the PL bundle experienced a peak relative elongation of $5.9\% \pm 3.4\%$ at 15° of flexion. The relative elongations at 0° and 45° of flexion were significantly ($P < 0.05$) smaller than those at 15° and 30° of flexion in both AM and PL bundles.

Multiple surface fiber bundles

Surface fiber bundle 4 at the anteromedial portion of the ACL was the longest fiber among all surface fiber bundles of the ACL at all flexion angles (Fig. 6A, B). The maximum length of this fiber under the no-load condition was 34.9 ± 3.6 mm at full extension, significantly longer compared to other flexion angles; and it was 35.5 ± 3.3 mm at 30° of flexion under full body weight. Surface bundle 7 on the posterolateral portion of the ACL was the shortest fiber on the surface of ACL. The length of this fiber was 21.8 ± 3.8 mm at full extension under the no-load condition and 16.2 ± 2.4 mm at 30° of flexion. The lengths of the eight surface fiber bundles of the ACL under no load and full body weight in all flexion angles are listed in Table 1. In general, the posterior fiber bundles are shorter than the anterior fiber bundles. This means that the AM and PL bundles have different behavior at low flexion angles.

There was a dramatic difference between the relative elongations among the surface fiber bundles (Fig. 6C). Surface fiber bundles at the anteromedial surface showed less relative elongation values compared to those at the posterolateral surface. The peak relative elongation of surface fiber bundle 4 was $5.0\% \pm 2.4\%$ under the full body weight at 30° of flexion. The peak relative elongation of surface fiber bundle 7 had a value of $13.4\% \pm 3.8\%$ at 30° of flexion in response to full body weight loading. Except in full extension, the relative elongation of this fiber bundle was significantly higher than all other fiber bundles at other flexion angles.

Discussion

This study investigated the elongation behavior of the ACL under increased axial tibial load of the knee at various flexion angles. The data demonstrated that the ACL elongated as the axial tibial load increased, as illustrated by previous studies.^{18,20} The data also showed that the ACL deformed in a nonhomogeneous manner. Each fiber bundle responded to the axial tibial load differently.

The relative elongation of the overall ACL reached >4.5% at 15° and 30° of flexion when the tibial load increased from no load (<10 N) to full body weight. Both AM and PL bundles also showed increases in relative elongations as the tibial load increased. The AM bundle showed peak relative elongation of 4.5% at 30°, and the PL bundle showed maximum relative elongation of 5.9% at 15° of flexion. The surface fiber bundles showed a more dramatic variation in relative elongations under the body weight loading applied to the tibia. In general, the bundles at the anteromedial surface showed less relative elongation than the bundles at the posterolateral surface of the ACL. At 30°, the posterolateral surface bundle 7 showed a relative elongation of >13% from no tibial load to full body weight tibial load, whereas surface fiber bundle 1 only had a relative elongation of approximately 3%.

Our previous in vivo studies indicated that the AM bundle of the ACL maintained maximum length between full extension to 45° of flexion and showed a reduction in length at higher flexion angles.²¹ The PL bundle showed maximum length in full extension and decreased in length as the knee flexed during a single leg lunge. In general, the current study showed similar length patterns of the AM and PL bundles with flexion. Our previous in vitro studies also demonstrated that the ACL carried a peak load, and ACL deficiency caused higher anterior tibial translation at low flexion angles when the knee is subject to simulated muscleloads.²⁸

Fleming et al.^{11,16,18} measured the ACL strain in its anterior portion using a DVRT that was installed on the ACL surface of living subjects. The strain was shown to decrease with flexion from 15° of flexion. During various activities (e.g., squatting, active flexion-extension) the peak strain was shown to be around 4% at 15° of flexion. Our data showed that, on average, the relative elongations of the AM surface bundle were >3% under full body weight at both 15° and 30° flexion angles and decreased at higher flexion angles. A direct comparison between these various studies is difficult as the in vivo loading conditions among these studies could not be controlled to be the same. Furthermore, the references for measuring relative elongations between these studies are different. For example, Fleming et al. determined that the reference length for measuring an anterior ACL strain was at 30° of flexion with an 8.8 N anterior shear load applied to the tibia using cadaveric knees,¹¹ whereas we used the length of the ligament under no load at each flexion angle as a reference.

Our data indicated that each bundle behaved differently even under the same loading conditions and at the same flexion angles. It may be necessary to determine a reference length for each interested fiber bundle. However, because of the complicated 3D geometry of the ACL, a unique reference length for each fiber bundle is difficult to determine using current technology. The fiber bundle lengths of the ACL changed with flexion angle even under the no-load conditions. Therefore, the relative elongation of this study at one flexion angle was calculated using the ligament length under the no-load condition (<10 N) at the same flexion angle as a reference. If the ACL bundle is slack under the no-load condition (i.e., the reference length, l_0 , is shorter than the actual reference length value), the relative elongation data calculated using the formula $e = (I - l_0)/l_0$ may overestimate the actual relative strain of the bundle. In contrast, if the ACL bundle is already in tension under the

no-load condition, the relative elongation could be underestimated. Also, if any interaction of the ACL and the PCL exists in the range of flexion of this study, the reported values for relative elongation of the surface fibers are underestimated. This point is worth investigating in future studies.

The data demonstrated different behavior of the ACL at different flexion angles even though the tibial load was controlled to be similar. Whereas the overall ACL showed peak relative elongation at 15° and 30° of flexion under full body weight, the AM bundle showed peak relative elongation at 30° and the PL bundle at 15°. Similar patterns were also seen among the eight ACL surface bundles, where all bundles showed peak relative elongations at 30° of flexion. Woo et al. demonstrated that in a uniaxial tensile test the ACL behaved differently when oriented in different flexion angles.⁴ The ACL was shown to be stiffer in tension at 30° of flexion. Different behavior of the ACL at different flexion angles indicated that the fiber recruitment of the ACL varies with flexion angles. It is interesting to note that, on average, the ACL and all surface fiber bundles showed peak relative elongation at around 30° of flexion, indicating that the ACL may experience larger deformation around this flexion angle. Consequently, the ACL properties might adapt to the loading conditions experienced at different flexion angles.

In general, the fiber bundles in the posterolateral portion of the ACL were shorter (~30% shorter) compared to the anteromedial portion. However, the posterior portion stretched more than the anterior portion and usually had higher relative elongations. This phenomenon may have important implications to surgical ACL reconstruction. Simulation of the ACL as a single bundle or double bundles may be insufficient to describe the complicated functional behavior of the ACL. It also points out the difficulty of determining truly “isometric” sites for tunnel placement using either single- or double-bundle reconstruction techniques. DeFrate et al.²⁹ and Li et al.³⁰ have quantitatively demonstrated that the length of the ligament has a profound effect on its stiffness. The stiffness increases with reduction of the ligament length. Surgical reconstruction of the ACL should take into consideration the length effect of the anteromedial and posterolateral portions of the ACL. Furthermore, it might be critically important to simulate the nonhomogeneous deformation of the ACL bundles using graft materials for ACL reconstruction.

There are several limitations in the current study that need to be improved in future investigations. The ligament length was calculated using a straight line connecting the two insertion points on the tibia and femur. This treatment might not be accurate to account for ACL impingement with the femoral notch at full extension of the knee. Furthermore, interaction of the ACL and PCL was not considered in the current study. Ignoring the impingement with femoral notch and interaction with the PCL would cause underestimation of ACL elongation using the straight-line model.

The relative elongation of the ACL was measured under full body weight applied to the tibia only from full extension to 45° of flexion. Beyond 45°, the subjects had difficulty applying full body weight to one knee and maintaining the flexion angle at the same time. Because of the experimental setup, these data thus represent only the quasi-static responses of the ACL. The relative elongation of the ACL under functional dynamic loading conditions, such as walking and stair climbing, should be investigated in the future.

Conclusions

This study investigated the relative elongation of the ACL when the knee was loaded under full body weight in living subjects. The data demonstrated that different ACL bundles behaved differently, but are not truly “reciprocal” in that one bundle does not shorten while

the other bundle lengthens. The fiber bundles at the posterior portion of the ACL are shorter than those at the anterior portion. However, the posterior fiber bundles experienced higher relative elongations than the anterior fiber bundles. Even though the overall relative elongations of the ACL might not be high, the posterior portion of the ACL might experience up to 13% relative elongation under full body weight. The data suggest that ACL biomechanics should be investigated in a three-dimensional manner. The data might provide some useful insight for improving ACL reconstruction techniques aimed at reproducing in vivo function of the ACL. They also suggest that current reconstruction techniques using single-bundle grafts or double-bundle grafts may not adequately restore the 3D deformation behavior of the ACL.

Acknowledgments

This research was supported by NIH grant R21AR051078. The technical assistance of Ramprasad Papannagari, Jeff Bingham, Dr. Samuel Van de Velde, Dr. Louis E. DeFrate, Dr. Kyung Wook Nha, and Angela Moynihan is greatly appreciated.

References

1. Mommersteeg TJ, Huijskes R, Blankevoort L, Kooloos JG, Kauer JM. An inverse dynamics modeling approach to determine the restraining function of human knee ligament bundles. *J Biomech.* 1997; 30:139–146. [PubMed: 9001934]
2. Sakane M, Fox RJ, Woo SL, Livesay GA, Li G, Fu FH. In situ forces in the anterior cruciate ligament and its bundles in response to anterior tibial loads. *J Orthop Res.* 1997; 15:285–293. [PubMed: 9167633]
3. Butler DL, Guan Y, Kay MD, Cummings JF, Feder SM, Levy MS. Location-dependent variations in the material properties of the anterior cruciate ligament. *J Biomech.* 1992; 25:511–518. [PubMed: 1592856]
4. Woo SL, Hollis JM, Adams DJ, Lyon RM, Takai S. Tensile properties of the human femur-anterior cruciate ligament-tibia complex: the effect of specimen age and orientation. *Am J Sports Med.* 1991; 19:217–225. [PubMed: 1867330]
5. Song Y, Debski RE, Musahl V, Thomas M, Woo SL. A three-dimensional finite element model of the human anterior cruciate ligament: a computational analysis with experimental validation. *J Biomech.* 2004; 37:383–390. [PubMed: 14757458]
6. Darcy SP, Kilger RH, Woo SL, Debski RE. Estimation of ACL forces by reproducing knee kinematics between sets of knees: a novel non-invasive methodology. *J Biomech.* 2006; 39:2371–2377. [PubMed: 16199046]
7. Mommersteeg TJ, Blankevoort L, Huijskes R, Kooloos JG, Kauer JM. Characterization of the mechanical behavior of human knee ligaments: a numerical-experimental approach. *J Biomech.* 1996; 29:151–160. [PubMed: 8849808]
8. Henning CE, Lynch MA, Glick KR Jr. An in-vivo strain gage study of elongation of the anterior cruciate ligament. *Am J Sports Med.* 1985; 13:22–26. [PubMed: 3976977]
9. Woo SL, Wu C, Dede O, Vercillo F, Noorani S. Biomechanics and anterior cruciate ligament reconstruction. *J Orthop Surg.* 2006; 1:2.
10. Ahmed AM, Burke DL, Duncan NA, Chan KH. Ligament tension pattern in the flexed knee in combined passive anterior translation and axial rotation. *J Orthop Res.* 1992; 10:854–867. [PubMed: 1403300]
11. Fleming BC, Beynon BD, Tohyama H, Johnson RJ, Nichols CE, Renström P, et al. Determination of a zero strain reference for the anteromedial band of the anterior cruciate ligament. *J Orthop Res.* 1994; 12:789–795. [PubMed: 7983554]
12. Beynon BD, Johnson RJ, Fleming BC, Renström PA, Nichols CE, Pope MH, et al. The measurement of elongation of anterior cruciate-ligament grafts in-vivo. *J Bone Joint Surg Am.* 1994; 76:520–531. [PubMed: 8150819]

13. Li G, Rudy TW, Sakane M, Kanamori A, Ma CB, Woo SL. The importance of quadriceps and hamstring muscle loading on knee kinematics and in-situ forces in the ACL. *J Biomech.* 1999; 32:395–400. [PubMed: 10213029]
14. Rudy TW, Livesay GA, Woo SL, Fu FH. A combined robotic/ universal force sensor approach to determine in situ forces of knee ligaments. *J Biomech.* 1996; 29:1357–1360. [PubMed: 8884481]
15. Li G, Zayontz S, Most E, DeFrate LE, Suggs JF, Rubash HE. In situ forces of the anterior and posterior cruciate ligaments in high knee flexion: an in vitro investigation. *J Orthop Res.* 2004; 22:293–297. [PubMed: 15013087]
16. Fleming BC, Beynnon BD, Nichols CE, Johnson RJ, Pope MH. An in vivo comparison of anterior tibial translation and strain in the anteromedial band of the anterior cruciate ligament. *J Biomech.* 1993; 26:51–58. [PubMed: 8423168]
17. Kanamori A, Zeminski J, Rudy TW, Li G, Fu FH, Woo SL. The effect of axial tibial torque on the function of the anterior cruciate ligament: a biomechanical study of a simulated pivot shift test. *Arthroscopy.* 2002; 18:394–398. [PubMed: 11951198]
18. Fleming BC, Renstrom PA, Beynnon BD, Engstrom B, Peura GD, Badger GJ, et al. The effect of weightbearing and external loading on anterior cruciate ligament strain. *J Biomech.* 2001; 34:163–170. [PubMed: 11165279]
19. Li G, Suggs J, Gill T. The effect of anterior cruciate ligament injury on knee joint function under a simulated muscle load: a three-dimensional computational simulation. *Ann Biomed Eng.* 2002; 30:713–720. [PubMed: 12108845]
20. Li G, DeFrate LE, Rubash HE, Gill TJ. In vivo kinematics of the ACL during weight-bearing knee flexion. *J Orthop Res.* 2005; 23:340–344. [PubMed: 15734246]
21. Jordan SS, DeFrate LE, Nha KW, Papannagari R, Gill TJ, Li G. The in vivo kinematics of the anteromedial and posterolateral bundles of the anterior cruciate ligament during weightbearing knee flexion. *Am J Sports Med.* 2007; 35:547–554. [PubMed: 17261571]
22. Bingham J, Li G. An optimized image matching method for determining in-vivo TKA kinematics with a dual-orthogonal fluoroscopic imaging system. *J Biomech Eng.* 2006; 128:588–595. [PubMed: 16813450]
23. Mochizuki T, Muneta T, Nagase T, Shirasawa S, Akita KI, Sekiya I. Cadaveric knee observation study for describing anatomic femoral tunnel placement for two-bundle anterior cruciate ligament reconstruction. *Arthroscopy.* 2006; 22:356–361. [PubMed: 16581446]
24. Harner CD, Baek GH, Vogrin TM, Carlin GJ, Kashiwaguchi S, Woo SL. Quantitative analysis of human cruciate ligament insertions. *Arthroscopy.* 1999; 15:741–749. [PubMed: 10524822]
25. Buoncristiani AM, Tjoumakaris FP, Starman JS, Ferretti M, Fu FH. Anatomic double-bundle anterior cruciate ligament reconstruction. *Arthroscopy.* 2006; 22:1000–1006. [PubMed: 16952731]
26. Li G, Wuerz TH, DeFrate LE. Feasibility of using orthogonal fluoroscopic images to measure in vivo joint kinematics. *J Biomech Eng.* 2004; 126:314–318. [PubMed: 15179865]
27. DeFrate LE, Papannagari R, Gill TJ, Moses JM, Pathare NP, Li G. The 6 degrees of freedom kinematics of the knee after anterior cruciate ligament deficiency: an in vivo imaging analysis. *Am J Sports Med.* 2006; 34:1240–1246. [PubMed: 16636348]
28. Yoo JD, Papannagari R, Park SE, DeFrate LE, Gill TJ, Li G. The effect of anterior cruciate ligament reconstruction on knee Joint kinematics under simulated muscle loads. *Am J Sports Med.* 2005; 33:240–246. [PubMed: 15701610]
29. DeFrate LE, van der Ven A, Gill TJ, Li G. The effect of length on the structural properties of an achilles tendon graft as used in posterior cruciate ligament reconstruction. *Am J Sports Med.* 2004; 32:993–997. [PubMed: 15150048]
30. Li G, DeFrate L, Suggs J, Gill T. Determination of optimal graft lengths for posterior cruciate ligament reconstruction: a theoretical analysis. *J Biomech Eng.* 2003; 125:295–299. [PubMed: 12751293]

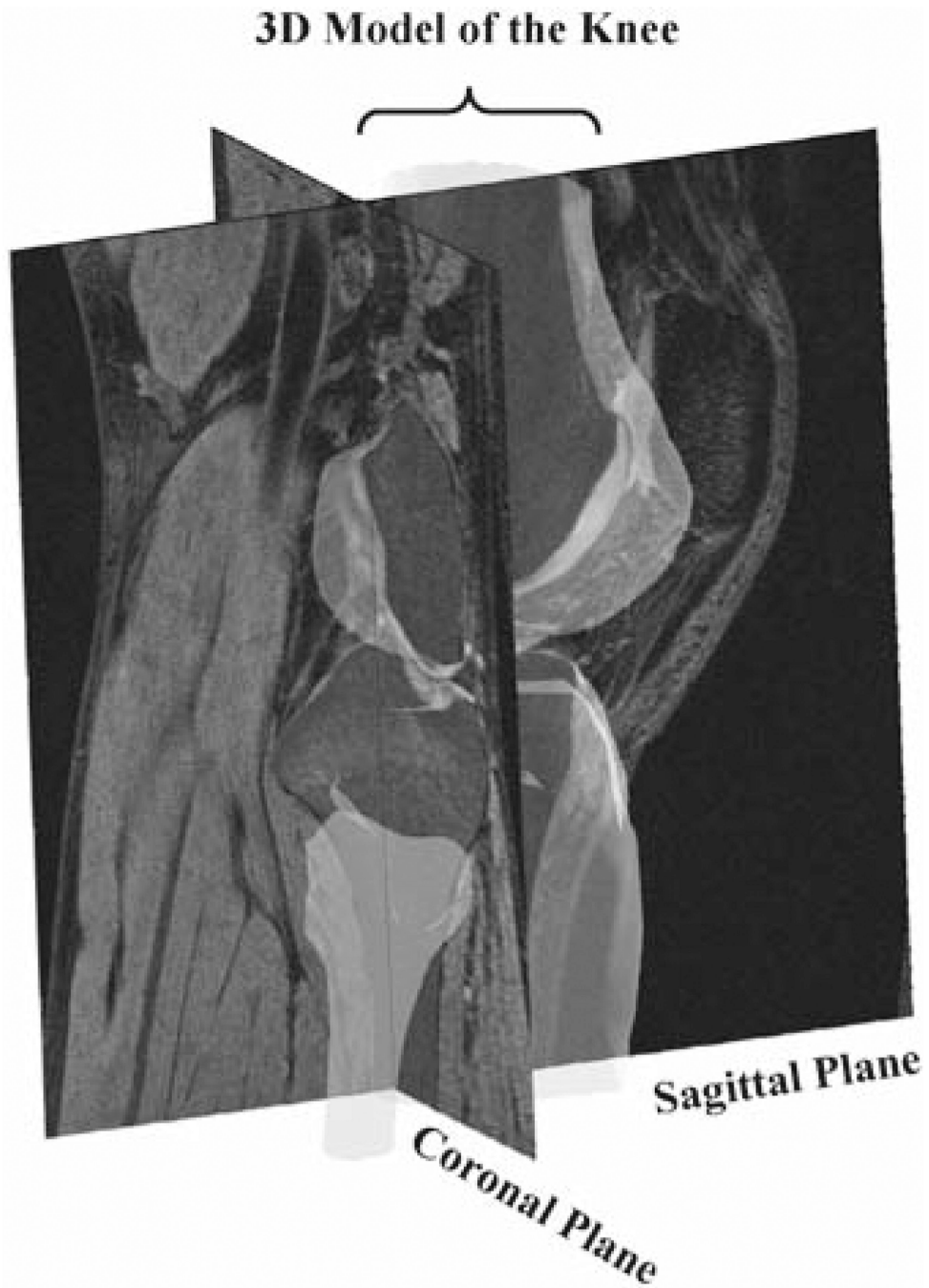


Fig. 1. Magnetic resonance (MR) images of a knee in the sagittal and coronal planes and construction of a three-dimensional (3D) knee model using magnetic resonance imaging (MRI)

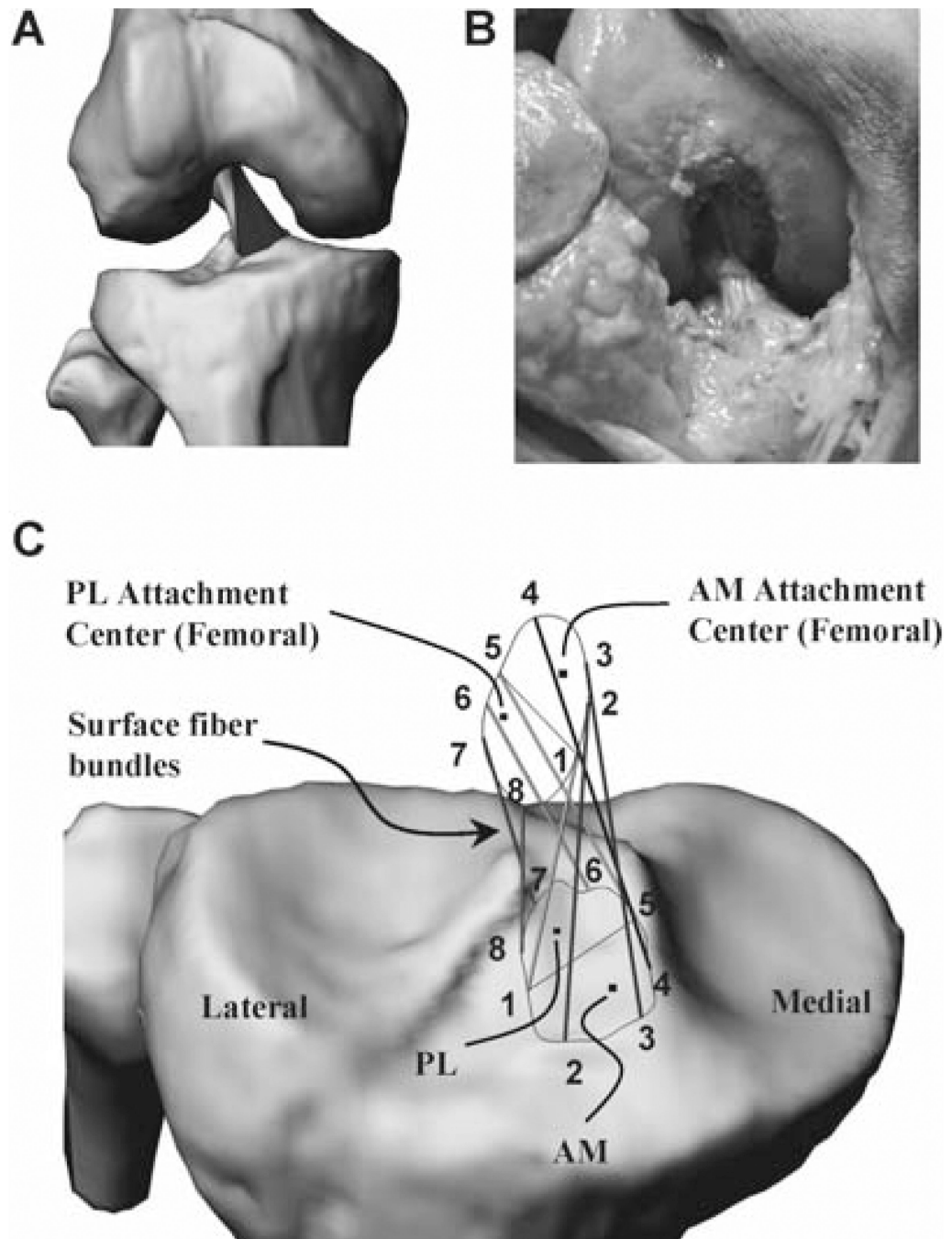


Fig. 2.
A Three-dimensional anterior cruciate ligament (ACL) model constructed from MR images.
B ACL configuration of a cadaveric knee. **C** Definition of ACL surface fiber bundles. *PL*, posterolateral; *AM*, anteromedial

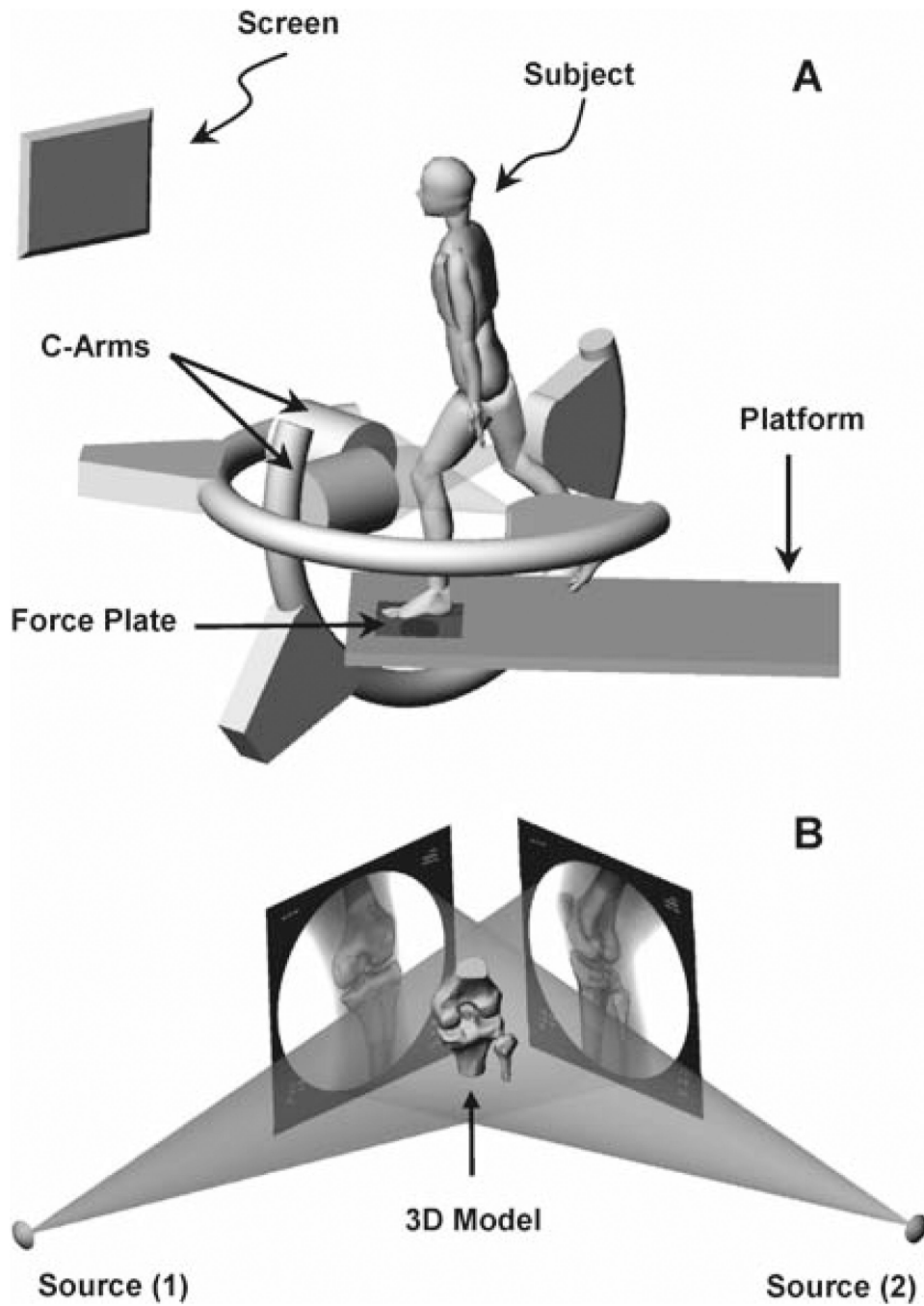


Fig. 3. **A** Dual fluoroscopic system for measuring joint position in space and a subject during a lunge activity. (From Jordan et al.,²¹ with permission) **B** Virtual dual fluoroscopic system constructed for reproducing the in vivo knee position in space

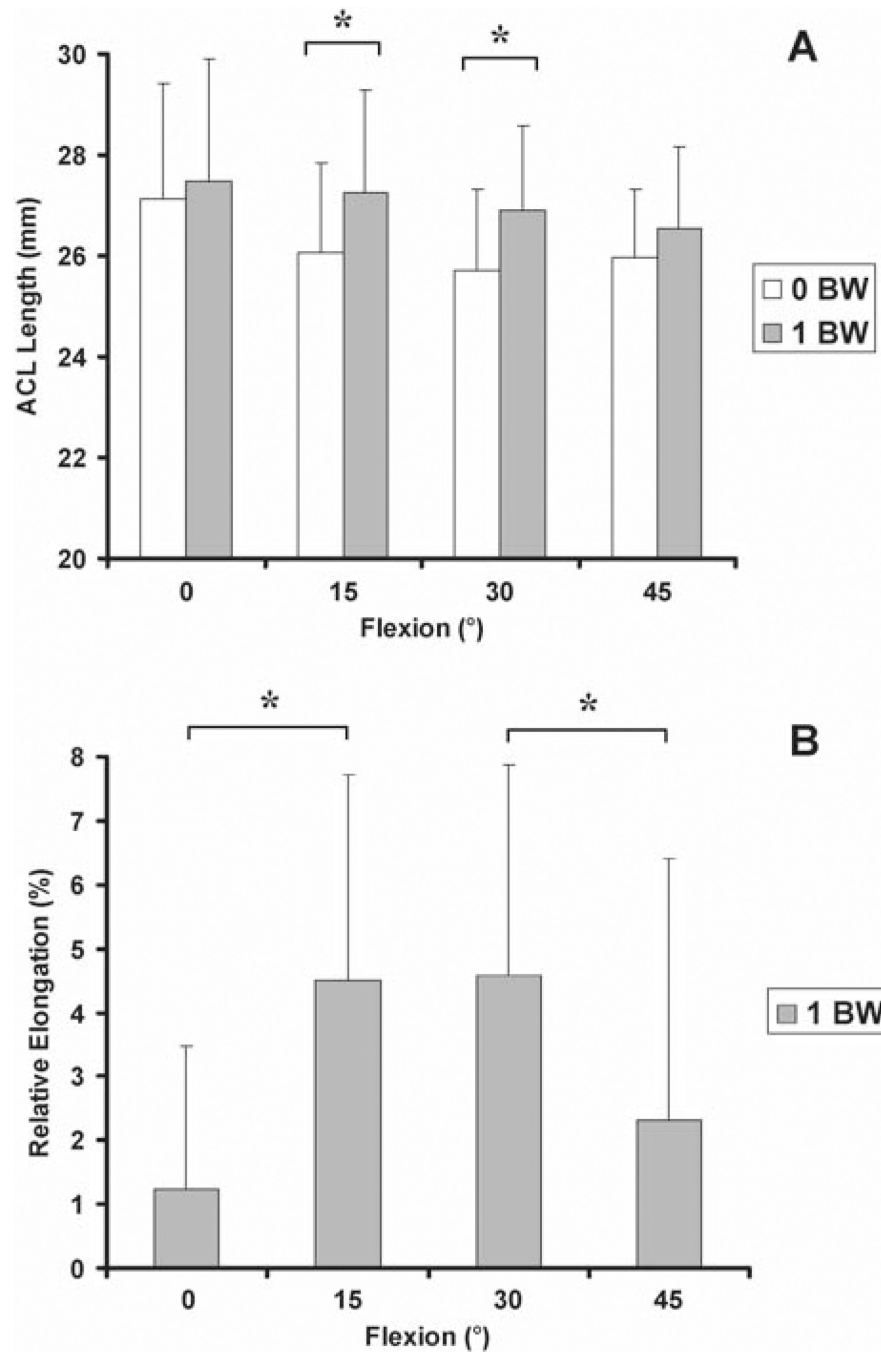


Fig. 4. **A** Length of the ACL central bundle when the knee is under no load and under full body load at various flexion angles. *BW*, body weight. **B** Relative elongation of the ACL central bundle in response to full body weight

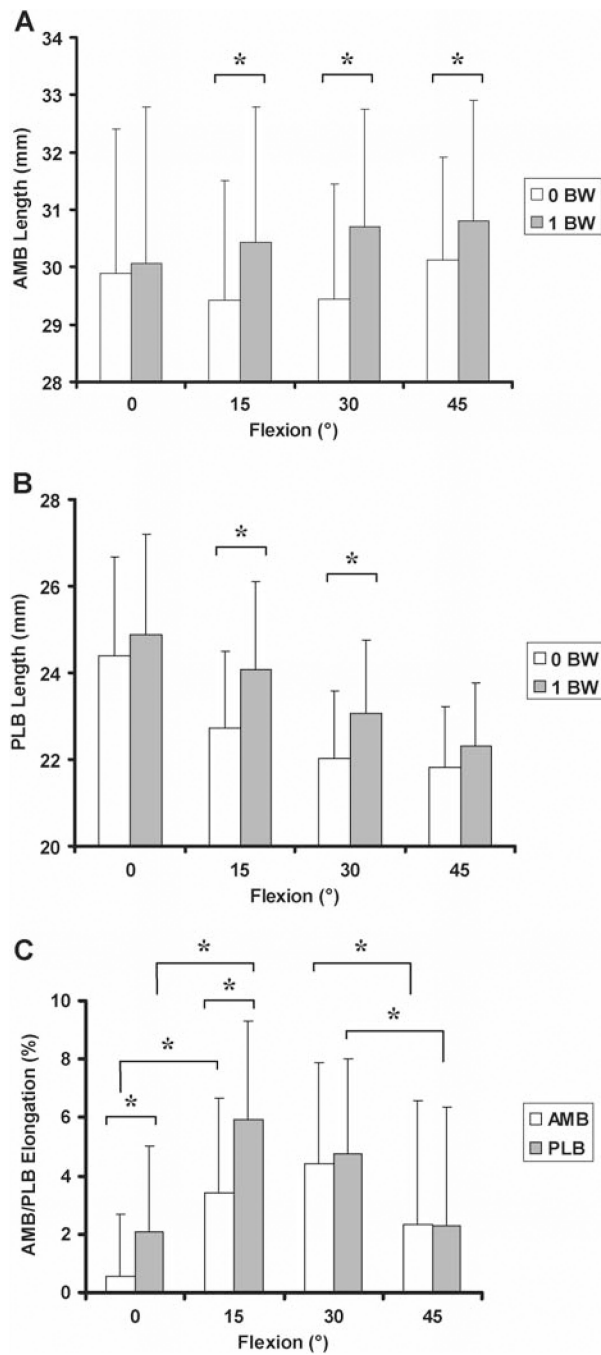
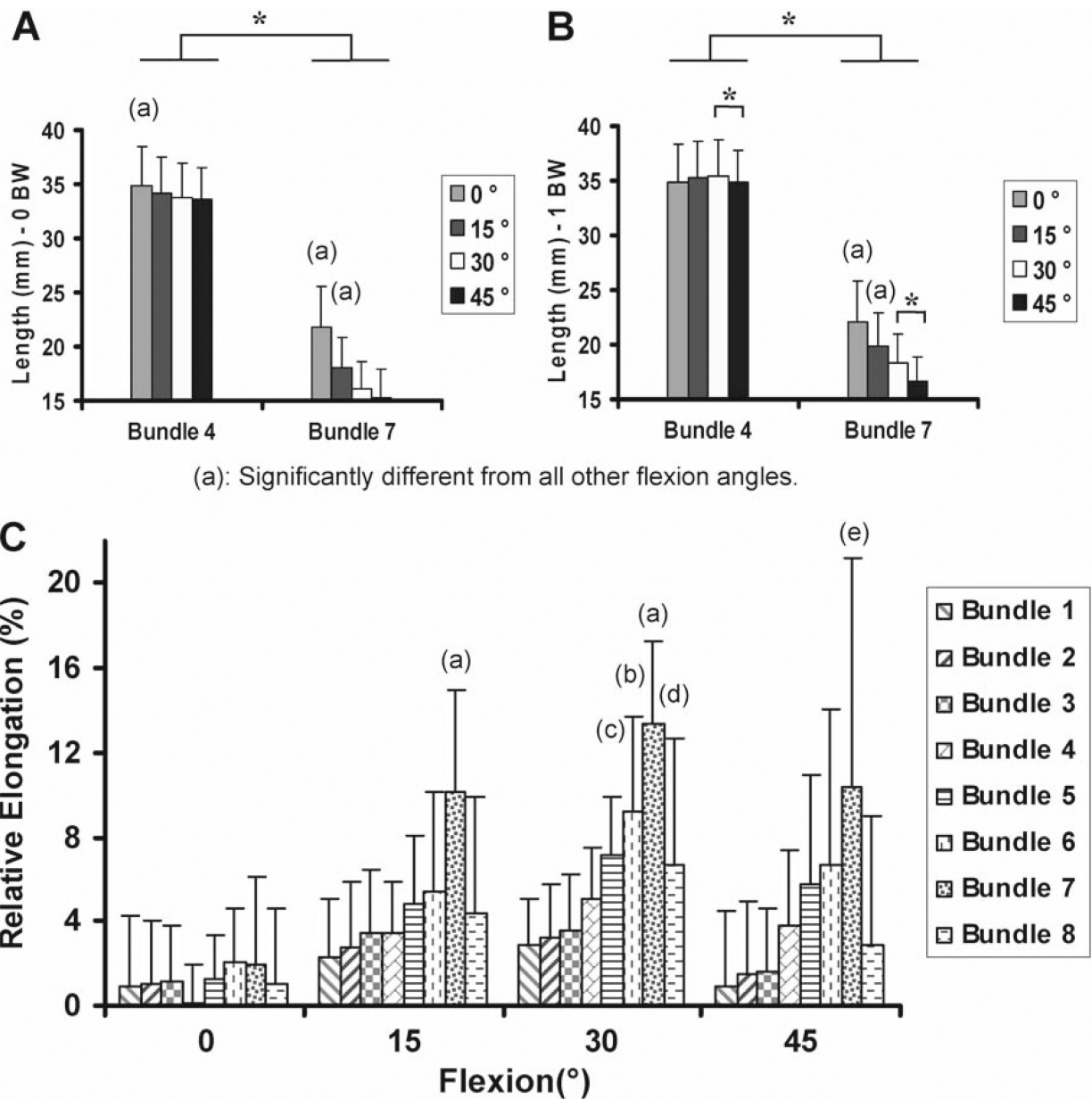


Fig. 5. Lengths of the (A) anteromedial bundle (*AMB*) and (B) posterolateral bundle (*PLB*) when the knee is under no load and at full body load at various flexion angles. C Relative elongation of the AM and PL bundles in response to full body weight



(a): Significantly different from all other flexion angles.

(a): Significantly different from all other bundles. (b): Significantly different from bundles 1 to 4. (c): Significantly different from bundles 1 to 3. (d): Significantly different from bundles 1 to 3 and 7. (e): Significantly different from bundles 1 to 4 and 8. (All are comparing at the same flexion angle)

Fig. 6. Lengths of the anterior surface bundle 4 and the pos- elongation of the eight ACL surface fiber bundles in response terior surface bundle 7 when the knee is under (A) no load to full body weight and (B) full body load at various flexion angles. C Relative elongation of the eight ACL surface fi ber bundles in response to full body weight

Table 1

Lengths of the eight surface fiber bundles of the anterior cruciate ligament ($n = 9$)

Bundle	0° ^a		15° ^a		30° ^a		45° ^a	
	0 BW	1.0 BW	0 BW	1.0 BW	0 BW	1.0 BW	0 BW	1.0 BW
1	25.5 ± 2.4	25.7 ± 2.0	25.5 ± 1.8	26.0 ± 1.9	25.9 ± 1.4	26.7 ± 1.7	27.3 ± 1.5	27.6 ± 1.6
2	30.2 ± 3.1	30.5 ± 3.1	30.2 ± 2.6	31.1 ± 2.6	30.8 ± 2.2	31.8 ± 2.5	32.1 ± 2.3	32.6 ± 2.5
3	32.6 ± 2.8	33.0 ± 2.7	32.4 ± 2.4	33.5 ± 2.4	32.8 ± 2.0	34.0 ± 2.4	33.8 ± 2.0	34.3 ± 2.6
4	34.9 ± 3.6	34.9 ± 3.4	34.1 ± 3.4	35.3 ± 3.4	33.8 ± 3.2	35.5 ± 3.3	33.6 ± 3.0	34.8 ± 3.0
5	31.2 ± 3.5	31.5 ± 3.6	29.1 ± 3.2	30.5 ± 3.1	27.7 ± 2.6	29.6 ± 2.7	26.8 ± 2.6	28.3 ± 2.3
6	26.1 ± 3.1	26.7 ± 3.2	23.1 ± 2.6	24.3 ± 2.5	20.9 ± 2.1	22.8 ± 2.1	19.8 ± 2.2	21.1 ± 1.8
7	21.8 ± 3.8	22.2 ± 3.7	18.1 ± 2.7	19.9 ± 3.0	16.2 ± 2.4	18.3 ± 2.6	15.2 ± 2.7	16.6 ± 2.2
8	21.1 ± 2.5	21.4 ± 2.6	19.3 ± 2.0	20.1 ± 2.1	18.5 ± 1.2	19.7 ± 1.4	18.8 ± 1.6	19.3 ± 1.5

Data are given as the mean ± SD

BW, body weight

^a Flexion angle